J. Iran. Chem. Soc., Vol. 7, No. 4, December 2010, pp. 917-933.

JOURNAL OF THE
Iranian
Chemical Society

Novel, Biologically Imperative, Highly Versatile and Planar Systems: Synthesis, Characterization, Electrochemical Behavior, DNA Binding and Cleavage Properties of Substituted β-Diketimine Copper(II) and Zinc(II) Complexes with Dipyrido(3,2-a:2′3,′-c)phenazine Ligand

N. Raman[a,*], R. Jeyamurugan[a], B. Rajkapoor[b] and L. Mitu[c]

[a]*Research Department of Chemistry, VHNSN College, Virudhunagar, India-626 001*

[b]*Department of Pharmacology, Sebha University, Sebha, Libya*-18758

[c]*Department of Physics and Chemistry, University of Pitesti, Pitesti, Romania-110 040*

(Received 16 November 2009, Accepted 16 February 2010)

Novel copper(II) and zinc(II) complexes of the type [ML(dppz)]Cl_2, [L = Schiff base derived from the condensation of 3-(3-phenyl-allylidene)-pentane-2,4-dione and para-substituted aniline; X = -NO_2 (L^1), -H (L^2), -OH (L^3) and -OCH_3 (L^4); dppz = dipyrido (3,2-a:2′3,′-c)phenazine] were synthesized and characterized by various analytical and spectral techniques. The physico-chemical studies and spectral data indicated that all the complexes were monomeric and cationic with square-planar geometry. Spectroscopic data and viscosity measurements showed that the complexes intercalated to DNA with large binding constants. The substituted groups such as -NO_2, -H, -OH and -OCH_3 in aniline moiety influenced the observed trend in the redox potentials of the complexes. The peak potential separation and formal potential of complexes were independent of sweep rate or scan rate (ν) indicating a quasireversible one-electron redox process. In all the cases, i_p was linear function of $\nu^{1/2}$, as expected for diffusion controlled process, and $i_{pa}/i_{pc} \approx 1$ at all sweep rates. It was found that the decrease in i_{pc} was due to the higher binding of copper complexes and slowly diffusing DNA. In the presence of a reducing agent like 3-mercaptopropionic acid (MPA), the chemical nuclease activity order of the copper complexes under dark reaction condition was -NO_2 > -H > -OH > -OCH_3. The hydrolytic cleavage of DNA by the zinc complexes was supported by the evidence from free radical quenching and T4 ligase ligation.

Keywords: β-Diketimine, Complexes, Dppz, DNA binding, DNA cleavage

INTRODUCTION

β-Diketimines, versatile ligand systems, have been long known to form complexes with almost every metal ion and metalloid. Condensation of the active methylene group of the β-diketone with an aldehydic group gives a non-enolisable Knoevenagel condensate, which can effectively react with amines to form Schiff bases [1]. Among the widely studied ligands, diimine compounds have attracted special attention due to their flexibility, facility of preparation, and ability to stabilize the oxidation states of the metal. Schiff base can coordinate with metal atom *via* nitrogen atom of C=N- double bond, leading to more stable complexes. Schiff base complexes are involved in specific activities of pharmacology and physiology. They have wide applications in various fields such as illness treatment, biochemical reaction and as biological regulators. Therefore, great interest is shown in their synthesis, structure, biological activity and practical application [2,3].

Molecules which are able to irreversibly modify nucleic acids have received considerable attention because of their potential applications as chemotherapeutic agents. Transition

*Corresponding author. E-mail: drn_raman@yahoo.co.in

metal complexes endowed with redox properties and DNA affinities have been developed as chemical nucleases. Typical examples of these DNA cleavers are iron-bleomycin, Fe(II)-EDTA, Mn(III)-porphyrin, Ni, Zn, Cu, Co, Rh and Ru complexes of phenanthroline or bipyridine [4-8]. All these complexes are able to mediate oxidative damage to nucleoebases and/or to the 2-deoxyribose moiety. Knowledge of their DNA oxidation mechanisms is highly useful to explore the potential application of these molecules as biological tools or therapeutic agents, since their toxic or therapeutic effects could be associated with their ability to produce DNA damage that is difficult to repair [9,10].

1,10-Phenanthroline(phen) is a versatile ligand, able to chelate copper to give mono-phen or bis-phen complexes in the oxidation states of +1 or +2 [11]. These complexes, in the presence of hydrogen peroxide, can efficiently cleave double-stranded DNA by oxidative attacks on C1′ and C4′ of 2-deoxyribose hydrogens by interacting within the minor groove. However, DNA cleavage efficiency of phen analogue complexes is less compared with the dppz analogue copper complexes due to the presence of the extended planar structure of the dppz ligands which greatly facilitate groove binding/stacking with base pairs.

Hence, we have synthesized a few mixed versatile ligand systems, Knoevenagel condensate β-diketones, as Schiff bases containing electron releasing/electron withdrawing groups and dppz and their copper(II) and zinc(II) complexes. An examination of their structure, spectral and redox properties as models for metalloproteins is essential in order to further address the structure-redox relationship. It is therefore of interest to carry out investigations on model compounds to find out how a ligand environment could affect the redox properties of the central metal and, thereby, the spectral ones. Particularly, we are interested in exploring the DNA binding and DNA cleavage activity of synthesized complexes. The findings would be helpful for understanding the binding mode of the complex to DNA. The study also lays a foundation for developing new and useful DNA probes and effective inorganic complex nucleases.

EXPERIMENTAL

Materials and Methods

All reagents and chemicals were procured from Merck products. Solvents used for electrochemical and spectroscopic studies were purified by standard procedures [12]. DNA was purchased from Bangalore Genei (India). Agarose (molecular biology grade) and ethidium bromide (EB) were obtained from Sigma (USA). Tris(hydroxymethyl)aminomethane-HCl (Tris-HCl) buffer solution was prepared using deionized and sonicated triply distilled water. The N,N-donor heterocyclic base, dipyrido[3,2-a:2’,3’-c]phenazine (dppz), was prepared by the literature procedure using 1,10-phenanthroline-5,6-dione as a precursor reacted with *o*-phenylenediamine [12,13].

Carbon, hydrogen and nitrogen analysis of the complexes were carried out on a CHN analyzer Calrlo Erba 1108, Heraeus. The infrared spectra (KBr discs) of the samples were recorded on a Perkin-Elmer 783 series FTIR spectrophotometer. The electronic absorption spectra in the 200-1100 nm were obtained on a Shimadzu UV-1601 spectrophotometer. ^{1}H and ^{13}C NMR spectra (300 MHz) of the ligands and their zinc complexes were recorded on a Bruker Avance DRX 300 FT-NMR spectrometer using $CDCl_3$ and DMSO-d_6 as solvents, respectively. Trimethylsilane was used as the internal standard. Fast atomic bombardment mass spectra (FAB-MS) were obtained using a VGZAB-HS spectrometer in a 3-nitrobenzylalcohol matrix. The X-band EPR spectra of the complexes were recorded at RT (300 K) and LNT (77 K) using DPPH as the g-marker. Molar conductance of the complexes (10^{-3} M) in N,N′-dimethylformamide (DMF) was measured at room temperature with a Deepvision Model-601 digital direct reading deluxe conductivity meter. Magnetic susceptibility measurements were carried out by employing the Gouy method at room temperature on powdered sample of the complex. $CuSO_4.5H_20$ was used as calibrant. Electrochemical measurements were performed on a CHI620C electrochemical analyzer with three electrode system of a glassy electrode as the working electrode, a platinum wire as auxiliary electrode and Ag/AgCl as the reference electrode. Solutions were deoxygenated by purging with N_2 prior to measurements. The metal content of the complexes was determined according to the literature method [14]. Chloride ion was determined gravimetrically as silver chloride. The purity of ligands and their complexes were evaluated by column and thin layer chromatography.

Synthesis of Ligands and Metal Complexes

Synthesis of 3-(3-phenyl-allylidene)-pentane-2,4-dione. The nonenolisable β-diketone was prepared by employing

the modified procedure reported earlier [15]. Pentane-2,4-dione (10 mmol) was mixed with 3-phenyl-propenal (10 mmol) and piperidine (0.2 ml), and the reaction mixture was stirred thoroughly for *ca*. 5 h with occasional cooling. Yellow colored crystalline solid was obtained after two weeks of being kept in the refrigerator. It was filtered, washed with ethanol followed by an excess of petroleum-ether to remove any unreacted reagent. Washing was `repeated two to three times and the compound was recrystallized from $CHCl_3$-petroleum ether mixture to give a pure yellow solid Knoevenagel condensate [3-(3-phenyl-allylidene)-pentane-2,4-dione]. It was used as the starting material for the preparation of Schiff base. Yield: 65%. IR (KBr pellet, cm^{-1}): 1718 ν(-C=O), 1570 ν(-HC=C). ^1H NMR (δ): (aromatic, 7H) 6.9-7.3 (m); (-C=CH-, 1H), 8.2 (d); ($-CH_3$), 2.3 (s). ^{13}C NMR (δ): 126.0-128.0 (C_1 to C_3), 138.4 (C_4), 129.0 (C_5), 125.7 (C_6), 146.9 (C_7), 145.2 (C_8), 197.5 (C_9), 24.5 (C_{10}). MS m/z (%): 215 $[M+1]^+$. Anal. Calcd. for $C_{14}H_{14}O_2$: C, 78.5; H, 6.7; Found: C, 78.1; H, 6.2 (%). λ_{max} (cm^{-1}) in EtOH, 37986.

Synthesis of Schiff base. The Schiff base was prepared by dissolving 3-(3-phenyl-allylidene)-pentane-2,4-dione (10 mmol) in ethanol and refluxed with substituted [X = $-NO_2$ (L^1), -H (L^2), -OH (L^3) and $-OCH_3$ (L^4)] aniline (20 mmol) in ethanol after the addition 0.5 g of anhydrous K_2CO_3 for *ca*. 6 h. The K_2CO_3 was filtered off from the reaction mixture. The dark brown solution was set aside to evaporate and the dark brown solid separated was filtered off and recrystallized from ethanol and dried *in vacuo*.

L^1. Yield: 54%. IR (KBr pellet, cm^{-1}): 1629 ν(-C=N); 1580 ν(-HC=C); 1480, 1324, 864 ν(-C-N ring str; $-NO_2$). ^1H NMR (δ): (aromatic) 6.8-7.2 (m); ($-CH_3$, 6H), 2.1 (s). ^{13}C NMR (δ): 125.0-127.6 (C_1 to C_5), 137 (C_6), 116 (C_7), 161.4 (C_8), 18.9 (C_9), 152.5 (C_{10}), 121.9 (C_{11}), 123.6 (C_{12}), 146.8 (C_{13}). MS m/z (%): 455 $[M+1]^+$. Anal. Calcd. for $C_{26}H_{22}N_4O_4$: C, 68.7; H, 4.9; N, 12.3; Found: C, 68.2; H, 4.9; N, 12.0 (%). λ_{max} (cm^{-1}) in EtOH, 46256, 27635.

L^2. Yield: 52%. IR (KBr pellet, cm^{-1}): 1586 ν(-HC=C-); 1632 ν(-C=N). ^1H NMR (δ, ppm): (aromatic) 6.9-7.3 (m); ($-CH_3$, 6H), 2.5 (s). ^{13}C NMR (δ, ppm): 125.6-128.2 (C_1 to C_5 and C_{13}), 137 (C_6), 116 (C_7), 158.6 (C_8), 17.6 (C_9), 148.5 (C_{10}), 120.9 (C_{11}), 129.9 (C_{12}). MS m/z (%): 365 $[M+1]^+$. Anal. Calcd. for $C_{26}H_{24}N_2$: C, 85.7; H, 6.6; N, 7.7; Found: C, 85.2; H, 6.6; N, 7.3 (%). λ_{max} (cm^{-1}) in EtOH, 41854, 28965.

L^3. Yield: 54%. IR (KBr pellet, cm^{-1}): 3434 ν(-OH); 1638 ν(-C=N); 1572 ν(-HC=C). ^1H NMR (δ, ppm): (aromatic) 6.9-7.5 (m); (-OH, 1H) 11.8 (s); ($-CH_3$, 6H), 2.3 (s). ^{13}C NMR (δ, ppm): 125.2-129.5 (C_1 to C_5), 137 (C_6), 116 (C_7), 159.6 (C_8), 14.7 (C_9), 139.2 (C_{10}), 123.8 (C_{11}), 120.4 (C_{12}), 152.6 (C_{13}). MS m/z (%): 397 $[M+1]^+$. Anal. Calcd. for $C_{26}H_{24}N_2O_2$: C, 78.6; H, 6.1; N, 7.1; Found: C, 78.1; H, 6.1; N, 7.0 (%). λ_{max} (cm^{-1}) in EtOH, 45298, 28269.

L^4. Yield: 47%. IR (KBr pellet, cm^{-1}): 1641 ν(-C=N); 1589 ν(-HC=C); 1284, 1086 ν(-C-O-C-). ^1H NMR (δ): (aromatic) 6.9-7.3 (m); ($-CH_3$, 6H), 2.4 (s); 3.7 ($-OCH_3$, 6H). ^{13}C NMR (δ): 125.0-128.0 (C_1 to C_5), 137 (C_6), 116 (C_7), 159.4 (C_8), 16.9 (C_9), 141.8 (C_{10}), 123.3 (C_{11}), 116.2 (C_{12}), 154.6 (C_{13}), 59.5 (C_{14}). MS m/z (%): 425 $[M+1]^+$. Anal. Calcd. for $C_{28}H_{28}N_2O_2$: C, 79.2; H, 6.7; N, 6.6; Found: C, 79.0; H, 6.7; N, 6.3 (%). λ_{max} (cm^{-1}) in EtOH, 42354, 28518

Synthesis of metal complexes. To a stirred ethanol solution of the above Schiff base(s) (5 mmol), a solution of copper/zinc chloride (5 mmol) in ethanol was added dropwise. After the reaction for 1 h at 70 °C, a solution of dppz (5 mmol) in ethanol was added. The reaction solution was refluxed for 2 h. After cooling the reaction mixture to an ambient temperature, the formed solid was filtered, washed with diethyl ether and finally dried *in vacuum*.

$[CuL^1(dppz)]Cl_2$. Yield: 42%. IR (KBr pellet, cm^{-1}): 1607 ν(-C=N); 1578 ν(-HC=C); 1508 ν(-C-N ring str.; dppz), 871, 749 ν(-C-H out of plane def.; dppz); 1476, 1328, 866 ν(-C-N str; $-NO_2$); 419 (M-N). MS m/z (%): 872 $[M+1]^+$. Anal. Calcd. for $CuC_{44}H_{32}N_8O_4Cl_2$: Cu, 7.3; C, 60.7; H, 3.7; N, 12.9; Found: Cu, 6.8; C, 60.5; H, 3.7; N, 12.4 (%). Λ_M 10^{-3} (ohm^{-1} cm^2 mol^{-1}) = 157.1. λ_{max} in EtOH, 44345, 35428, 17815, 18547. μ_{eff} (BM): 1.81.

$[CuL^2(dppz)]Cl_2$. Yield: 51%. IR (KBr pellet, cm^{-1}): 1615 ν(C=N); 1587 ν(-HC=C); 1524 ν(C-N ring str.; bpy); 859, 737 ν(C-H out of plane def.; dppz); 432 (M-N). MS m/z (%): 782 $[M+1]^+$. Anal. Calcd. for $CuC_{44}H_{34}N_6Cl_2$: Cu, 8.1; C, 67.7; H, 4.4; N, 10.8; Found: Cu, 7.8; C, 67.2; H, 4.4; N, 7.5 (%). Λ_M 10^{-3} (ohm^{-1} cm^2 mol^{-1}) = 149.0 λ_{max} (cm^{-1}) in EtOH, 40816, 29876, 16152, 18956. μ_{eff} (BM): 1.86.

$[CuL^3(dppz)]Cl_2$. Yield: 38%. IR (KBr pellet, cm^{-1}): 1615 ν(-C=N); 1573 ν(-HC=C); 1516 ν(-C-N ring str.; dppz), 742, 861 ν(-C-H out of plane def.; dppz); 3432 ν(-OH); 424 (M-N). MS m/z (%): 814 $[M+1]^+$. Anal. Calcd. for $CuC_{44}H_{34}N_6O_2Cl_2$:

Cu, 7.8; C, 65.0; H, 4.2; N, 10.3; Found: Cu, 7.6; C, 64.8; H, 4.2; N, 10.0 (%). Λ_M 10^{-3} (ohm^{-1} cm^2 mol^{-1}) = 142.3. λ_{max} (cm^{-1}) in EtOH, 41216, 31785, 17478, 19123. μ_{eff} (BM): 1.84.

[CuL^4(dppz)]Cl$_2$. Yield: 49%. IR (KBr pellet, cm^{-1}): 1613 ν(-C=N); 1585 ν(-HC=C); 1278, 1081, ν(-C-O-C-); 1515 ν(-C-N ring str.; dppz); 739, 864 ν(C-H out of plane def.; dppz); 412 (M-N). MS m/z (%): 842 $[M+1]^+$. Anal. Calcd. for $CuC_{46}H_{38}N_6O_2Cl_2$: Cu, 7.6; C, 65.7; H, 4.6; N, 10.0; Found: Cu, 7.2; C, 65.2; H, 4.5; N, 9.6 (%). Λ_M 10^{-3} (ohm^{-1} cm^2 mol^{-1}) = 137.3. λ_{max} (cm^{-1}) in EtOH, 41256, 30129, 17153, 18489. μ_{eff} (BM): 1.83.

[ZnL^1(dppz)]Cl$_2$. Yield: 47%. IR (KBr pellet, cm^{-1}): 1612 ν(-C=N); 1577 ν(-HC=C); 1509 ν(-C-N ring str.; dppz), 871, 745 ν(-C-H out of plane def.; dppz); 1475, 1321, 860 ν(-C-N str; -NO_2); 416 (M-N). ^{1}H NMR (δ): (aromatic) 6.9-7.2 (m); (-CH_3, 6H), 2.3 (s); (dppz, 2H), 9.6 (dd); (dppz, 2H), 9.3 (dd); (dppz, 2H), 8.6 (s), (dppz, 2H), 7.5 (dd). MS m/z (%): 874 $[M+1]^+$. Anal. Calcd. for $ZnC_{44}H_{32}N_8O_4Cl_2$: Zn, 7.5; C, 60.5; H, 3.7; N, 12.8; Found: Zn, 7.1; C, 60.0; H, 3.6; N, 12.5 (%). Λ_M 10^{-3} (ohm^{-1} cm^2 mol^{-1}) = 139.9. λ_{max} (cm^{-1}) in EtOH, 42365, 32659. μ_{eff} (BM): diamagnetic.

[ZnL^2(dppz)]Cl$_2$. Yield: 42%. IR (KBr pellet, cm^{-1}): 1608 ν(-C=N); 1584 ν(-HC=C); 1519 ν(-C-N ring str.; dppz); 852, 744 ν(-C-H out of plane def.; dppz); 419 (M-N). ^{1}H NMR (δ): (aromatic) 6.8-7.1 (m); (-CH_3, 6H), 2.6 (s); (dppz, 2H), 9.8 (dd); (dppz, 2H), 9.4 (dd); (dppz, 2H), 8.3 (s), (dppz, 2H), 7.8 (dd). MS m/z (%): 784 $[M+1]^+$. Anal. Calcd. for $ZnC_{44}H_{34}N_6Cl_2$: Zn, 8.4; C, 67.5; H, 4.4; N, 10.7; Found: Zn, 8.0; C, 67.0; H, 4.1; N, 10.7 (%). Λ_M 10^{-3} (ohm^{-1} cm^2 mol^{-1}) = 152.7 λ_{max} (cm^{-1}) in EtOH, 40924, 29898. μ_{eff} (BM): diamagnetic.

[ZnL^3(dppz)]Cl$_2$. Yield: 43%. IR (KBr pellet, cm^{-1}): 1619 ν(-C=N); 1574 ν(-HC=C); 1517 ν(-C-N ring str.; dppz); 847, 742 ν(-C-H out of plane def.; dppz); 3431 ν(-OH); 435 (M-N). ^{1}H NMR (δ): (aromatic) 6.8-7.1 (m); ν(-OH, 1H), 11.4; (-CH_3, 6H), 2.3 (s); (dppz, 2H), 9.7 (dd); (dppz, 2H), 9.5 (dd); (dppz, 2H), 8.5 (s), (dppz, 2H), 7.8 (dd). MS m/z (%): 816 $[M+1]^+$. Anal. Calcd. for $ZnC_{44}H_{34}N_6O_2Cl_2$: Zn, 8.0; C, 64.8; H, 4.2; N, 10.3; Found: Zn, 7.6; C, 64.3; H, 4.2; N, 10.0 (%). Λ_M 10^{-3} (ohm^{-1} cm^2 mol^{-1}) = 144.7. λ_{max} (cm^{-1}) in EtOH, 41984, 33287. μ_{eff} (BM): diamagnetic.

[ZnL^4(dppz)]Cl$_2$. Yield: 53%. IR (KBr pellet, cm^{-1}): 1619 ν(-C=N); 1583 ν(-HC=C); 1276, 1080 ν(-C-O-C-); 1521 ν(-C-N ring str.; dppz), 853, 742 ν(-C-H out of plane def.; dppz); 439 (M-N). ^{1}H NMR (δ): (aromatic) 7.0-7.4 (m); (-OCH_3, 6H), 3.6(s); (-CH_3, 6H), 2.3 (s); (dppz, 2H), 9.9 (dd); (dppz, 2H), 9.6 (dd); (dppz, 2H), 8.5 (s), (dppz, 2H), 7.7 (dd). MS m/z (%): 844 $[M+1]^+$. Anal. Calcd. for $ZnC_{46}H_{38}N_6O_2Cl_2$: Zn, 7.8; C, 65.5; H, 4.5; N, 9.9; Found: Zn, 7.5; C, 65.3; H, 4.5; N, 9.5 (%). Λ_M 10^{-3} (ohm^{-1} cm^2 mol^{-1}) = 148.3. λ_{max} (cm^{-1}) in EtOH, 42548, 31457. μ_{eff} (BM): diamagnetic.

DNA Binding and Cleavage Experiments

All the experiments involving the interaction of the complexes with Calf thymus (CT) DNA were carried out in Tris-HCl buffer (50 mM Tris-HCl, pH 7.2) containing 5% DMF at room temperature. A solution of CT DNA in the buffer gave a ratio of UV absorbance at 260 and 280 nm of about 1.89:1, indicating the CT DNA being sufficiently free from protein. The CT DNA concentration per nucleotide was determined by absorption spectroscopy using the molar absorption coefficient of 6600 M^{-1} cm^{-1} at 260 nm [16].

Absorption spectroscopic studies. Absorption titration experiment was performed by keeping the concentration of the metal complex as constant at 50 μM while varying the concentration of the CT DNA within 40-400 μM. While measuring the absorption spectrum, an equal amount of CT DNA was added to both the complex solution and the reference solution to eliminate the absorbance of CT DNA itself. From the absorption data, the intrinsic binding constant K_b was determined from the plot of $[DNA]/(\varepsilon_a-\varepsilon_f)$ *vs*. [DNA] using Eq. (1):

$$[DNA]/(\varepsilon_a-\varepsilon_f) = [DNA]/(\varepsilon_b-\varepsilon_f) + [K_b(\varepsilon_b-\varepsilon_f)]^{-1} \quad (1)$$

where [DNA] is the concentration of CT DNA in base pairs. The apparent absorption coefficients ε_a, ε_f and ε_b correspond to $A_{obsd.}/[M]$, the extinction coefficient for the free metal(II) complex and extinction coefficient for the metal(II) complex in the fully bound form, respectively [17]. K_b is given by the ratio of slope to the intercept.

Electrochemical methods. Cyclic voltammetry and Differential pulse voltammogram studies were performed on a CHI620C electrochemical analyzer with three electrode system of glassy carbon as the working electrode, a platinum wire as auxiliary electrode and Ag/AgCl as the reference

electrode. Solutions were deoxygenated by purging with N_2 prior to measurements. The freshly polished glassy electrode was modified by transferring a droplet of 2 µl of 2.5×10^{-3} M of CT DNA solution onto the surface, followed by air drying. Then the electrode was rinsed with distilled water. Thus, a CT DNA-modified gold electrode was obtained.

Viscosity measurements. Viscosity experiments were carried on an Ostwald viscometer, immersed in a thermostated water-bath maintained at a constant temperature at 30.0 ± 0.1 °C. CT DNA samples of approximately 0.5 mM were prepared by sonicating in order to minimize complexities arising from CT DNA flexibility [18]. Flow time was measured with a digital stopwatch three times for each sample and an average flow time was calculated. Data were presented as $(\eta/\eta^0)^{1/3}$ *vs.* the concentration of the metal(II) complexes, where η is the viscosity of CT DNA solution in the presence of the complex, and η^0 is the viscosity of CT DNA solution in the absence of the complex. Viscosity values were calculated after correcting the flow time of buffer alone (t_0), $\eta = (t - t_0)/t_0$ [19].

Photo-induced DNA cleavage experiment. The extent of cleavage of super-coiled (SC) pUC19 DNA (33.3 µM, 0.2 µg) to its nicked circular (NC) form was determined by agarose gel electrophoresis in 50 mM Tris-HCl buffer (pH 7.2) containing 50 mM NaCl. For photo-induced DNA cleavage studies, the reactions were monitored under illuminated conditions using UV sources at 360 nm. After exposure to light, each sample was incubated for 1 h at 37 °C and analyzed for the photo-cleaved products using gel electrophoresis as discussed below. The inhibition reactions for the "chemical nuclease" took place under dark conditions by adding reagent distamycin (50 µM)/DMSO (4 µl), prior to the addition of each complex and the reducing agent 3-mercaptopropionic acid (MPA). The inhibition reactions for the photo-induced DNA occurred at 360 nm using reagents NaN_3 (100 µM)/DMSO (4 µl), prior to the addition of each complex. For D_2O experiment, the solvent was used for dilution of the sample to 18 µl. The sample, after incubation for 1 h at 37 °C in a dark chamber, was added to the loading buffer containing 0.25% bromophenol blue, 0.25% xylene cyanol, 30% glycerol (3 µl) and the solution was finally loaded on 0.8% agarose gel containing 1 µg ml^{-1} ethiodium bromide. Electrophoresis was carried out in a dark chamber for 3 h at 50 V in Tris-acetate-EDTA buffer. Bands were visualized by UV light and photographed.

Hydrolytic DNA cleavage experiment. The 25 µl total volume of a mixture of 77 µM pUC 19 DNA with zinc complexes of 50 µM in 50 mM Tris-HCl buffer (pH 7.2) containing 50 mM NaCl was incubated for 30 min at 37 °C. To eliminate the effect of the oxidative species which results from the oxygen dissolved in the solution due to the hydrolysis reaction, the incubation of all samples was performed under anaerobic conditions such as deoxygenated and highly purified water, isolation of air, and in nitrogen atmosphere. The hydrolytic reactions were quenched by the addition of 4 µl TBE (89 mM Tris, 89 mM boron hydroxide, 2 mM EDTA) sample buffer containing xylene cyanol and bromophenol blue. The electrophoresis of DNA cleavage products was performed on 0.8% agarose gel. The gels were run at 50 V for 45 min in 0.01 M pH 7.2 NaH_2PO_4 and Na_2HPO_4 buffer. To perform simple kinetic analysis, the electrophoresis bands were visualized by staining in an ethidium bromide solution and photographed on UV tansilluminator at 360 nm.

Ligation experiment on the DNA by zinc complexes. First, the linear DNA was isolated from the pUC 19 DNA cleavage products provided by zinc complexes. Then, in each parallel experiment the 25 µl total volume of the mixture, containing 2 µl ligation buffer, 1 µl 0.1 M ATP, 4 µl 40% PEG and 3 Weiss units T4 DNA ligase, reacted with the linear DNA for 24 h at room temperature. The ligation products were monitored by the electrophoresis and visualized by staining in an ethidium bromide solution.

RESULTS AND DISCUSSION

Synthetic routes for the preparation of different compounds are depicted in the Scheme (Supplementary). The synthesized ligands and their complexes were found to be stable in air. The ligands were soluble in common organic solvents, but their complexes were soluble only in DMF and DMSO.

Infrared Spectra

The IR spectra of the complexes were compared with the IR spectra of the ligand in order to detect the changes that might have taken place. The ν(C=N) band present in the ligands is shifted to lower frequency by *ca.* 20 cm^{-1} on

complexation [17]. Coupled with this, the absence of a band above 1641 cm^{-1} [20], characteristic of ν(-C=O) in 3-(3-phenyl-allylidene)-pentane-2,4-dione, suggests the condensation of the keto groups. The free -OH group of the ligand L^3 vibrated at *ca.* 3435 cm^{-1} [20] does not show any significant shift on complex formation. Other bands observed at 847-871, 737-749 cm^{-1} (δ(-C-H) deformation) and 1508-1524 cm^{-1} (δ(-C-N) stretching band) after coordination, signify that phen ring of dppz complexes is coordinated to the central metal ion through nitrogen. The new band observed in the region 410-439 cm^{-1} for all the complexes is assigned to the M-N vibration.

Molar Conductivity

The complexes are found to be of 1:2 electrolytic natures at 10^{-3} M DMF solution, implying the non-coordination of chloride anion to the central metal ion. The presence of counter (chloride) ion is confirmed from Volhard's test. The elemental analytical data for the metal complexes also agree with the calculated values showing that the complexes exhibit 1:2 metal/ligand ratio.

Magnetic Moments and Electronic Spectra

The free ligands exhibit two intense bands in 46256-41854 and 28965-27635 cm^{-1} region due to $\pi\rightarrow\pi^*$ and $n\rightarrow\pi^*$ transitions [21], respectively. In all metal complexes, the absorption bands at 44345-40816 and 29876-35428 cm^{-1} due to $\pi\rightarrow\pi^*$ and $n\rightarrow\pi^*$ transitions that are observed in the spectra of the free ligands L^1, L^2, L^3 and L^4 are shifted to blue or red frequencies which indicate the coordination of the ligands with metal ions. The electronic spectra of Cu(II) complexes show two broad, low-intensity shoulder bands in the visible region, around 17815-16152 and 19213-18956 cm^{-1}, which are assigned to $^2B_{1g}\rightarrow{}^2A_{1g}$ and $^2B_{1g}\rightarrow{}^2E_g$ transitions, respectively. The electronic spectral data suggest a square-planar geometry around the Cu(II) ion. The observed magnetic moment of the Cu(II) complexes (1.81-1.86 B.M) at room temperature indicates the non-coupled mononuclear complexes of magnetically diluted d^9 system with S = 1/2 spin-state square-planar structure. The monomeric nature of the complexes is further supported by the microanlytical and FAB mass spectral data. The electronic absorption spectra of the diamagnetic Zn(II) complexes show IR bands at 40924-42548 and 29898-33287 cm^{-1} which are assigned to intra- ligand charge transfer transitions [22].

^{1}H NMR Spectra of Zinc Complexes

The NMR spectra of ligands and their diamagnetic Zn(II) complexes were recorded in DMSO-d_6. In ^{1}H NMR, the aromatic region is a set of mutiplets in the range of 6.8-7.8 ppm for all the ligands and their Zn(II) complexes. The phenolic -OH proton for L^3 ligand and its zinc complexes was observed as a singlet *ca.* 11.8 and 11.4 ppm, respectively. This indicates that phenolic -OH group did not take part in the complexation. ^{1}H NMR spectra of aliphatic methyl protons exhibit 2.1-2.6 ppm for all the Schiff base ligands and their Zn(II) complexes. In dppz complexes, the additional peaks observed at 9.6-9.9, 9.3-9.6, 8.3-8.5 and 7.5-7.8 ppm, assigned to dipyrido phenazine protons, suggest that dppz nitrogen atom is coordinated to Zn(II) ion. The peaks of 6.8-7.1 ppm are assigned to phenyl protons.

Mass Spectra

The FAB-mass spectra of synthesized ligands and their complexes were recorded and the obtained molecular ion peaks confirm the proposed formulae. The mass spectrum of L^3 ligand shows M+1 peak at m/z 397 (15.6%) corresponding to $[C_{26}H_{24}N_2O_2]^+$ ion. Also, the spectrum exhibits fragments at m/z 107, 77 and 66 corresponding to $[C_6H_5NO]^+$, $[C_6H_5]^+$ and $[C_5H_6]^+$, respectively. The mass spectrum of $[CuL^3(dppz)]Cl_2$ shows peaks at 814 and 815 with 19.8 and 15.7% abundances, respectively. The peak at 814 probably represents the molecular ion peak of the complex and the other peaks are isotopic species. The strongest peaks (base beak) at m/z 397 and 283 represent the stable species $C_{26}H_{24}N_2O_2$ and $C_{18}H_{10}N_4$, respectively. Furthermore, the spectrum exhibits the fragments at m/z 107, 77 and 66 corresponding to $[C_6H_5NO]^+$, $[C_6H_5]^+$ and $[C_5H_6]^+$, respectively. The m/z of all the fragments of ligands and their complexes confirms that the stoichiometry of the complexes is of $[ML(dppz)]Cl_2$ type. This is further supported by the mass spectra of all the complexes. The observed peaks are in good agreement with their empirical formulae as microanalytical data show. Thus, the mass spectral data reinforce the conclusion drawn from the analytical and conductance values.

EPR Spectral Study

To obtain further information about the stereochemistry

Table 1. The Spin Hamiltonian Parameters of Cu(II) Complexes in DMSO at 300 K and 77 K

Complexes	g-Tensor			$A \times 10^{-4}$ (cm^{-1})			α^2	β^2	G
	$g_{\parallel}$	$g_{\perp}$	g_{iso}	$A_{\parallel}$	$A_{\perp}$	A_{iso}			
$[CuL^1(dppz)]Cl_2$	2.22	2.06	2.11	152.3	49.4	83.7	0.70	1.06	3.79
$[CuL^2(dppz)]Cl_2$	2.20	2.05	2.10	149.6	51.8	84.4	0.67	1.01	4.17
$[CuL^3(dppz)]Cl_2$	2.23	2.06	2.12	157.2	54.0	88.4	0.73	1.09	3.96
$[CuL^4(dppz)]Cl_2$	2.19	2.05	2.10	145.1	48.2	80.5	0.65	1.01	3.96

and the site of the metal ligand bonding and to determine the magnetic interaction in the metal complexes, the X-band EPR spectra of all copper(II) complexes were recorded in DMSO at liquid nitrogen temperature and at room temperature. The spin Hamiltonian parameters of the complexes were calculated and are summarized in Table 1. The EPR spectra of copper(II) complexes at room temperature show one intense absorption band in the high field and is isotropic due to the tumbling motion of the molecules (Fig. 1). However, these complexes at liquid nitrogen temperature show four well-resolved peaks with low intensities in the low field region and one intense peak in the high field region (Fig. 1). From the spectral analytical data, it is deduced that $A_{\parallel}$ (145-158) > $A_{\perp}$ (48-54); $g_{\parallel}$ (2.19-2.23) > $g_{\perp}$ (2.05-2.06) > 2.0027, which support the $d_{x^2-y^2}$ as the ground state, characteristic of square-planar geometry and axially symmetric. Further, in an axial symmetry, the g-values are related by the expression, $G = (g_{\parallel} - 2.0027)/(g_{\perp} - 2.0027)$, which measure the exchange interaction between the copper centers in polycrystalline solid. According to Hathaway [23,24], the *G* values which fall within the range 3.67-4.00 for all copper complexes, indicate negligible exchange interaction of Cu-Cu in the complexes.

The degree of geometrical distortion is ascertained by the parameter $g_{\parallel}/A_{\parallel}$ ($A_{\parallel}$ in cm^{-1}) with the values less than 140 cm^{-1} associated with the square-planar structures, whereas higher values indicate distortion towards tetrahedron [24]. For the present copper complexes, the $g_{\parallel}/A_{\parallel}$ values, found in the range of 142-151 cm^{-1}, are in agreement with significant deviation from planarity which is further confirmed by the bonding parameter α^2 whose value is less than unity.

The covalency parameters α^2 (covalent in-plane σ-bonding) and β^2 (covalent in-plane π-bonding) were calculated

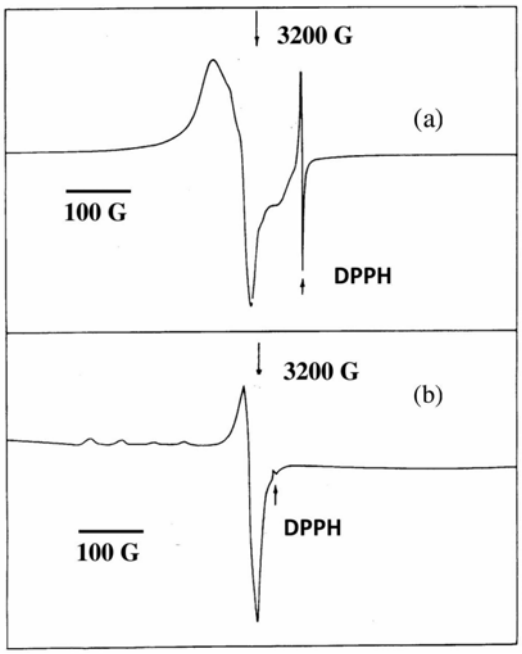

Fig. 1. EPR spectrum of $[CuL^1(dppz)]Cl_2$ in DMSO solution at (a) 300 K (b) 77 K.

using the following equations [23]. If $\alpha^2 = 1.0$, it indicates complete ionic character, whereas if $\alpha^2 = 0.5$, it denotes 100% covalent bonding, assuming negligible small values of the overlap integral.

$$\alpha^2 = (A_{\parallel}/0.036) + (g_{\parallel} - 2.0027) + 3/7\,(g_{\perp} - 2.0027) + 0.04$$

$$\beta^2 = (g_{\parallel} - 2.0027)\,(E/-8\lambda\alpha^2)$$

where $\lambda = -828$ cm^{-1} for free copper ion and *E* is electronic

transition energy. From Table 1, the α^2 and β^2 values indicate that there is a substantial interaction in the in-plane σ-bonding whereas the in-plane π-bonding is almost ionic. The lower value of α^2 compared to β^2 indicates that the in-plane σ-bonding is more covalent than in-plane π-bonding. These data are congruent with other reported values [23]. Based on these observations, a square-planar geometry is proposed for the complexes. The EPR study of the copper(II) complexes has provided supportive evidence to the conclusion obtained on the basis of electronic spectra and magnetic moment value.

Based on the above analytical and spectral data, the structures of the ligands and their complexes are shown in Fig. 2 and Fig. 3, respectively.

DNA Binding Studies

Electronic spectral studies. Absorption titration was used to monitor the interaction of the complexes with CT DNA. In general, a complex bound to DNA through intercalation usually results in hypochromism and blue shift of the absorption band due to strong stacking interaction between aromatic chromophore of the complex and the base pairs of the DNA. Intense absorption bands, observed near 300 nm in the synthesized complexes, are attributed to their LMCT transition involving the heterocyclic base and the metal ion. On increasing the CT DNA concentration, the hypochromism was found to increase with a blue shift in the UV band of the complexes (Fig. 4 and Supplementary). In order to compare the binding strength of the complexes with CT DNA, the intrinsic binding constants K_b were obtained by monitoring the changes in absorbance for the complexes with increasing concentration of DNA. K_b was obtained from the ratio of slope to the intercept from the plot of $[DNA]/(\varepsilon_a-\varepsilon_f)$ *vs*. [DNA]. The K_b values of copper and zinc complexes are shown in Table 2. The high K_b value for all the complexes is due to the presence of extended planar structure of the dppz ligands which greatly facilitate groove binding/stacking with the base pairs. The binding strength of the synthesized complexes with DNA is shown in the following order: $-NO_2 > -H > -OH > -OCH_3$.

Electrochemical behavior. The cyclic voltammmograms of all the copper and zinc complexes were recorded in DMF at room temperature. Typical CV behaviour of $[CuL^1(dppz)]Cl_2$ in the absence and presence of CT DNA is shown in Fig. 5. In the absence of DNA, the limiting peak potential separations

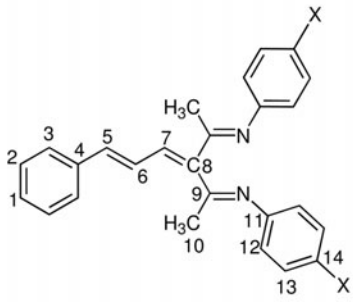

where X = $-NO_2$ (L^1), -H (L^2), -OH (L^3) and $-OCH_3$ (L^4)

Fig. 2. Structure of ligands.

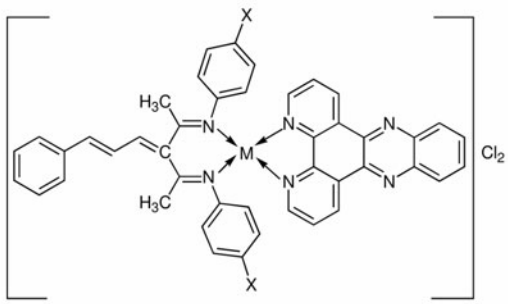

where X = $-NO_2$ (L^1), -H (L^2), -OH (L^3) and $-OCH_3$ (L^4)
M = Cu(II) and Zn(II)

Fig. 3. Structure of complexes.

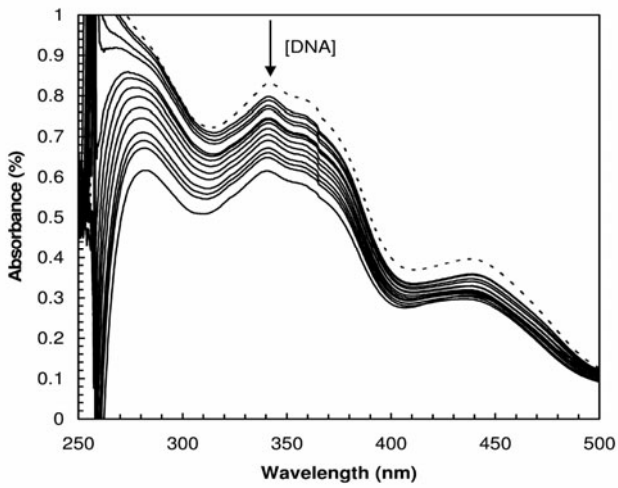

Fig. 4. Electronic absorption spectra of $[CuL^3(dppz)]Cl_2$ in the absence (dash line) and presence (dark line) of increasing amounts of DNA.

Table 2. Absorption Spectral Properties of Synthesized Complexes

SI. No	Complexes	λ_{max} (nm)		$\Delta\lambda$	%H	$K_b \times 10^5$
		Free	Bound	(nm)		(M^{-1})
1	$[CuL^1(dppz)]Cl_2$	341.8	335.6	6.2	29	8.4
2	$[CuL^2(dppz)]Cl_2$	339.0	333.4	5.6	19	8.0
3	$[CuL^3(dppz)]Cl_2$	334.5	331.2	3.3	11	3.2
4	$[CuL^4(dppz)]Cl_2$	336.4	332.1	4.3	12	4.1
5	$[ZnL^1(dppz)]Cl_2$	337.5	334.0	4.5	24	2.4
6	$[ZnL^2(dppz)]Cl_2$	342.3	337.2	5.1	16	3.5
7	$[ZnL^3(dppz)]Cl_2$	332.4	330.1	2.3	8	1.8
8	$[ZnL^4(dppz)]Cl_2$	335.7	333.3	2.4	6	2.1

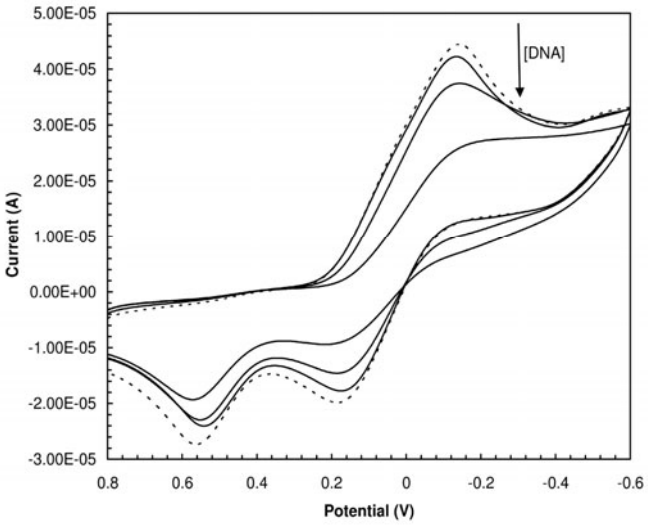

Fig. 5. Cyclic voltammogram of $[CuL^1(dppz)]Cl_2$ both in the absence (dash line) and presence (dark line) of different concentration of DNA. Supporting electrolyte, 50 mM NaCl, 5 mM Tris-HCl, pH = 7.2. Scan rate 100 mV s^{-1}.

(ΔEp) for all the copper complexes in the range 98-334 mV clearly indicate that these redox couples are quasi-reversible. The i_{pa}/i_{pc} values of all the copper complexes were found to be less than unity, clearly confirming one electron transfer in redox process. The quasi-reversible copper(II)/copper(I) redox couple was not altered on scanning at different sweep rates, showing that the redox peak current intensity increases on higher scan rates (Fig. 6 and supplementary). The cathodic peak current was found to be proportional to the square root of the scan rates indicating the the charge transfer processes were diffusion controlled, which is confirmed by the linearity of the i_{pc} *vs.* $\nu^{1/2}$ plot passing through the origin. The substitution of groups such as $-NO_2$, -H, -OH and $-OCH_3$ in aniline influences the observed trend in the half wave redox potentials (0.018-0.339 V) of the complexes. This illustrates the nuclease activity of copper complexes, as their Cu(II) and Cu(I) forms are involved in the proposed cleavage mechanism (Scheme 1). Thus, they are close to that of cleavage active copper-dppz complexes, suggesting that all of them should display significant nuclease activity.

The addition of an excess of DNA causes the peak current of the CV waves for the reduction of +2 to +1 form of copper complexes and anodic waves on the reverse scan diminish considerably. The cathodic peak current (i_{pc}) is decreased to *ca*. 16-58% in the absence of DNA. Additionally, the potentials, Epc and Epa, both are shifted to more positive values, equivalent to a shift in the formal potential of the Cu(II)/Cu(I) couple, $E^{0'}$ (taken as average of Epc and Epa), of 14-21 mV. The limiting shift of polarographic $E_{1/2}$ by differential pulse voltammetry (DPV) is 36-42 mV in the presence of very large excess of DNA. The peak potential separations (ΔEp = |Epc - Epa| and peak shapes, |Epc - Ep/2|) are independent of DNA concentration with changing the sweep rate ($10 \leq \nu \leq 100$ mV s^{-1}) indicating a quasi-reversible one electron redox process. In all the cases i_{pc} is linear function of $\nu^{1/2}$, as expected for diffusion controlled process and $i_{pa}/i_{pc} < 1$ at all sweep rate and concentration of DNA. The shift of the redox potential of the complexes in the presence of

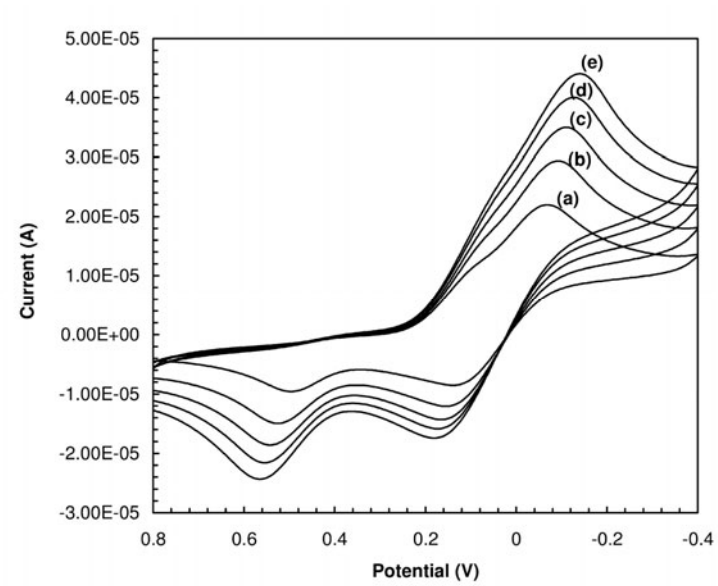

Fig. 6. Cyclic voltammograms of $[CuL^1(dppz)]Cl_2$ in DMF *vs*. Ag/AgCl with TBAP as supporting electrolyte at scan rate (a) 20, (b) 40, (c) 60, (d) 80 and (e) 100 mV s^{-1}.

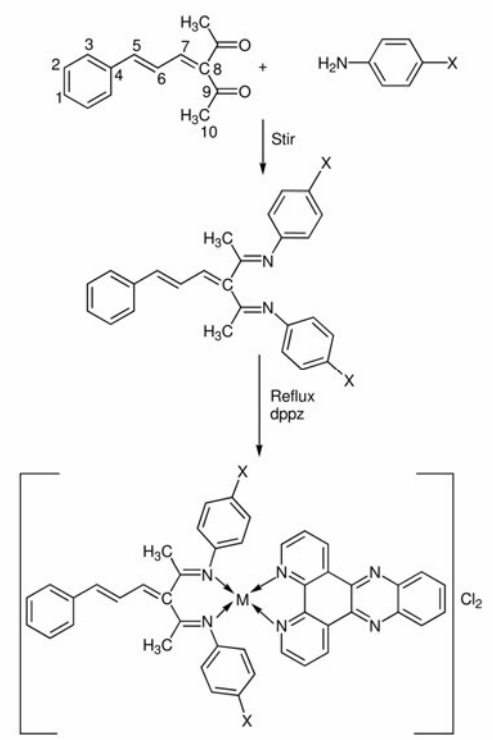

where X = $-NO_2$ (L^1), -H (L^2), -OH (L^3) and $-OCH_3$ (L^4) M = Cu(II) and Zn(II)

Scheme 1. The outline of the syntheses of metal complexes

DNA to more negative values indicates a binding interaction between the complexes and DNA that makes the complexes less readily reducible. The drop of the voltammetric current in the presence of CT DNA can be attributed to diffusion of metal complexes bound to the large, slowly diffusing DNA molecule and not to an increase in the solution viscosity. We have performed CV experiments on a mixture of complexes which intercalate between the DNA base pairs. The decreased extents of the peak currents observed for the complexes upon the addition of DNA may indicate that the electron-withdrawing group containing the complexes possess higher DNA-binding affinity than other complexes.

CV peak potentials of all copper complexes, both in the absence and presence of DNA, were found to be independent of sweep rate (ν), over the ranges 20-100 mV s^{-1}, somewhat smaller ΔEp with Epc and Epa independent of sweep rate. At a higher sweep rate (500 mV s^{-1}), and in the presence of DNA, slight broadening of ΔEp (Supplementary) was observed. This is possibly due to the onset of kinetic complication as well as a slight dependence of Ep on sweep rate (Epc = 0.123 V at 100 mV s^{-1} and [DNA] = 2.5×10^{-3} M, while Epc = 0.099 V at 500 mV $s^{-1}$and [DNA] = 2.5×10^{-3} M).

Typical DPV behavior of $[CuL^1(dppz)]Cl_2$ in the absence and presence of CT DNA is shown in Fig. 7. The measured $E_{1/2}$ values from DPV experiment are in good agreement with those determined from CV experiments. The net shift in $E_{1/2}$ can be used to estimate the ratio of equilibrium constant for the binding of the +2 to +1 ion to DNA for copper complexes. This is analogous to the treatment of the association of small molecules with micelles [25] and DNA [26]. For a Nernstein electron transfer in a system in which both the oxidized and reduced forms associate with third species in solution (DNA), Scheme 1 can be applied. Here, Cu^{2+} and Cu^{+} represent the oxidized and reduced forms of the metal complexes and Cu^{2+}-DNA and Cu^{+}-DNA denote the binding of copper complex to the DNA molecule. $E_f^{o'}$ and $E_b^{o'}$ are the formal potentials of Cu(II)/Cu(I) couple in the free and bound form, respectively. K_{2+} and K_{+} are the corresponding equilibrium constants for the binding of each oxidation to DNA yields, for a one-electron redox process

$$E_b^{o'} - E_f^{o'} = 0.0591 \log(K_{+}/K_{2+})$$

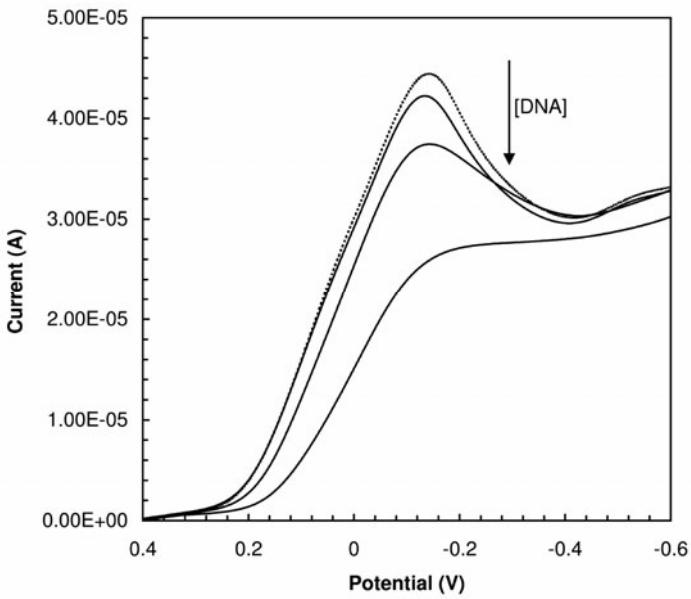

Fig. 7. Difference pulse voltammogram of $[CuL^1(dppz)]Cl_2$ both in the absence (dash line) and presence (dark line) of different concentration of DNA. Supporting electrolyte, 50 mM NaCl, 5 mM Tris-HCl, pH = 7.2.

Thus, K_+/K_{2+} values (Table 3) for electron-withdrawing group, containing copper complex were less than unity suggesting the preferential stabilization of Cu(II) form. However, and interestingly enough, we observed the ratio of binding constant for -OH and $-OCH_3$ group substituted complexes was approximately unity suggesting that each oxidant state interacts with DNA to the same extent.

The formal potential ($E_{1/2}$) of all the copper complexes is essentially unaffected by the presence of DNA. However, a little change in $E_{1/2}$ occurs after the addition of large amount of DNA (R = 40). For all the copper complexes, in the absence of DNA, i_{pc} is linear with $v^{1/2}$ for different sweep rates, with zero intercept within the error of the measurement. From this, the diffusion coefficient for copper complexes is obtained from the following equation

$$i_p = (2.69 \times 10^8)kn^{3/2}AD^{1/2}Cv^{1/2}$$

The slope of the i_{pc} - $v^{1/2}$ plot decreases with increasing R = [DNA]/[Complex], indicating a reduction in the apparent diffusion coefficient of the complexes as concentration of DNA increased. The value of apparent diffusion coefficient of copper complexes is given in Table 3. Thus, the apparent diffusion coefficient decreases with increasing the concentration of DNA. The diffusion coefficient of the free copper complex D_f, was obtained from the $i_{pc}/v^{1/2}$ data ($10 \leq v \leq 100$ mV s^{-1}) as 0.042-5.8 × 10^{-17} cm^2 s^{-1}. In the presence of DNA, the apparent diffusion coefficient of the bound copper complex D_b, obtained from differential pulse voltammetry, was 0.02-1.1 × 10^{-19} cm^2 s^{-1}. Typical voltammetric data of copper complexes at different DNA concentrations, given in terms of the relative concentration, R, and the concentration of DNA where R = [DNA]/[complex], are summarized in Table 3.

These results demonstrate that rather straight-forward electrochemical methods could be employed to characterize the intercalative interaction between metal complexes or electro active species and DNA. The electrochemical oxidation and reduction of selected bound species on DNA can also be carried out and favorable circumstances may allow strand scission in the DNA.

The electrochemical behaviour of all the zinc complexes in the absence of DNA shows only cathodic potential corresponding to Zn(II)/Zn(0). The cathodic peak appears to be the positive potential of 0.806-0.948 V range corresponding to the two-electron reduction of Zn(II) complexes. The addition of CT DNA to the zinc complexes solution results in a shift of cathodic peak potentials to more negative values and a decrease of the cathodic currents. The shift of the cathodic potential of the complexes in the presence of DNA to more negative values indicates a binding interaction between the complexes and DNA that makes the complexes less readily reducible. The drop of the voltammetric currents in the presence of CT DNA could be attributed to the diffusion of metal complexes bound to higher and slowly diffusing DNA molecule. The decreased extents of the peak currents observed for the complexes upon the addition of DNA might be indicative of the fact that copper complexes possess more DNA-binding affinity than do zinc complexes. Typical voltammetric data of zinc complexes at different DNA concentrations are summarized in Table 4. Peak potentials of zinc complexes were independent of sweep rate (50-500 mV s^{-1}) and ΔEp values were in between 63 and 76 mV.$E_{1/2}$ values were determined from the DPV peak potential (Ep) by the

Table 3. Electrochemical Parameters of Interaction of DNA with Copper Complexes

SI. No	Complexes	ΔEp (V)		$E_{1/2}$ (V)		Decrease of i_{pc} (%)	i_{pa}/i_{pc}		K_+/K_{2+}	Diffusion coefficient (cm^2 s^{-1})	
		Free	Bound	Free	Bound		Free	Bound		Free (D_f)	Bound (D_b)
1	$[CuL^1(dppz)]Cl_2$	-0.336	-0.302	0.020	0.046	58	0.45	0.08	0.84	5.8×10^{-17}	1.1×10^{-19}
2	$[CuL^2(dppz)]Cl_2$	-0.245	-0.229	0.383	0.389	24	0.89	0.74	0.90	2.2×10^{-17}	3.6×10^{-20}
3	$[CuL^3(dppz)]Cl_2$	-0.167	-0.192	0.055	0.018	19	0.50	0.36	0.98	3.9×10^{-18}	2.6×10^{-20}
4	$[CuL^4(dppz)]Cl_2$	-0.159	-0.133	0.171	0.178	16	0.76	0.61	0.12	4.2×10^{-19}	2.2×10^{-21}

relation $E_{1/2} = Ep + \Delta E/2$, where $E_{1/2}$ is the equivalent of the average of Epc and Epa in CV experiments and ΔE is the pulse amplitude (-50 mV). These $E_{1/2}$ values are in good agreement with those determined from CV experiments.

Differential pulse voltammogram of the Zn(II) complexes exhibits a negative potential shift along with significant decrease of current intensity during the addition of increasing amounts of DNA. This indicates that zinc ions stabilized the duplex (GC pairs) by intercalation. Hence, the complexes of the electroactive species (Zn(II)) with DNA, the electrochemical reduction reaction can be divided as follows:

$$Zn^{2+}\text{-DNA} \rightleftharpoons Zn^{2+} + \text{DNA}$$

$$Zn^{2+} + 2e^- \rightleftharpoons Zn^0$$

The dissociation constant (K_d) of the Zn(II)-DNA complex was obtained using the following equation:

$$i_p^2 = \frac{K_d}{[DNA]}(i_{po}^2 - i_p^2) + i_{po}^2 - [DNA] \quad (3)$$

where K_d is dissociation constant of the complex Zn(II)-DNA, i^2_po and i^2_p are reduction current of Zn(II) in the absence and presence of DNA respectively. The low dissociation constant values (Table 4) of Zn(II) ions are indispensable for structural stability of the complexes of Zn(II)-DNA which participate in the replication, degradation and translation of genetic material of all species.

Viscosity measurements. To further clarify the nature of the interaction between the complexes and DNA, viscosity measurements were carried out. In the absence of crystallographic structural data, hydrodynamic measurements, which are sensitive to length change (*i.e.*, viscosity and sedimentation) of DNA, are regarded as the least ambiguous and the most critical test of binding mode in solution. A classical intercalation mode results in lengthening the DNA helix, as base pairs are separated to accommodate the binding ligand, leading to the increase of DNA viscosity [27]. The effects of the complexes, together with ethidium bromide (EB) on the viscosity of CT DNA are shown in Fig. 8. It was found that the viscosity of DNA increased steadily with increasing the concentration of the complex, which is similar to that of classical intercalator ethidium bromide [28]. The increased degree of viscosity, which may depend on its affinity to DNA, follows the order of EB > $-NO_2$ > -OH > -H > $-OCH_3$. This demonstrates that the complexes and EB bind to DNA similarly, *i.e.*, the classical intercalation mode. The significant increase in viscosity of the complexes is obviously due to the partial insertion of the ligand between the DNA base pairs leading to an increase in the separation of base pairs at intercalation sites, hence an increase in overall DNA contour length [29].

DNA Cleavage Studies

Chemical nuclease activity. The DNA cleavage of the ligand alone is inactive in the presence and absence of any external agents. The results indicate the importance of the metal in the complex for observing the chemical nuclease activity. The oxidative cleavage of DNA in the presence of a reducing agent 3-mercaptopropionic acid (MPA, 5 mM) was studied by gel electrophoresis using supercoiled (SC) pUC19 DNA (0.2 l g, 33.3 l M) in 50 mM Tris-HCl/50 mM NaCl buffer (14 lL, pH 7.2) and the copper(II) complexes (50 l M) (Fig. 9 and Supplementary). The ‘‘chemical nuclease’’ activity follows the order: $-NO_2$ > -H > -OH > $-OCH_3$. Control

Table 4. Electrochemical Parameters for the Interaction of DNA with Zinc Complexes

SI. No.	Complexes	Ep (V)		i_{pc} (μA)		$K_d \times 10^{-10}$ (M)
		Free	Bound	Free	Bound	
1	$[ZnL^1(dppz)]Cl_2$	0.948	0.939	0.54	0.38	6.2
2	$[ZnL^2(dppz)]Cl_2$	0.892	0.886	0.56	0.43	5.8
3	$[ZnL^3(dppz)]Cl_2$	0.854	0.845	0.51	0.44	3.1
4	$[ZnL^4(dppz)]Cl_2$	0.806	0.795	0.48	0.40	1.8

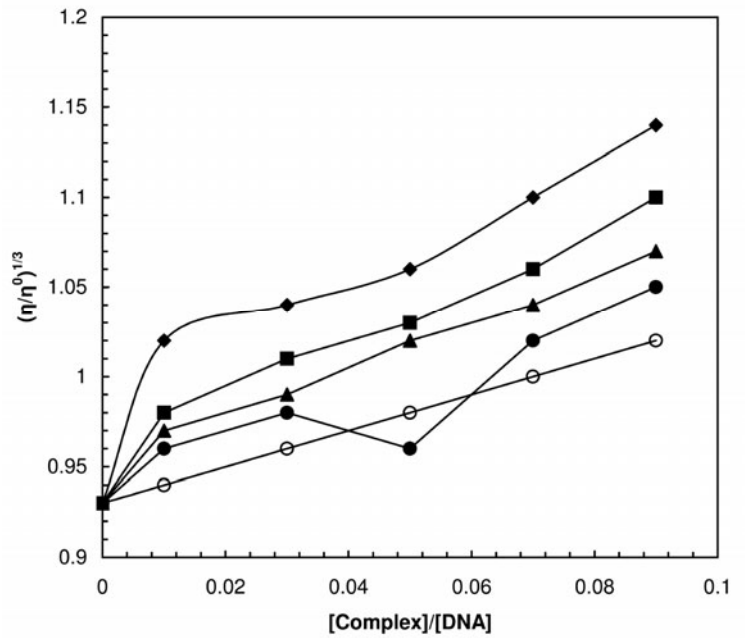

Fig. 8. The effect of EB (◆) $[CuL^1(dppz)]Cl_2$, (■) $[CuL^2(dppz)]Cl_2$, (▲) $[CuL^3(dppz)]Cl_2$, (●) $[CuL^4(dppz)]Cl_2$, (○) on the viscosity of DNA.

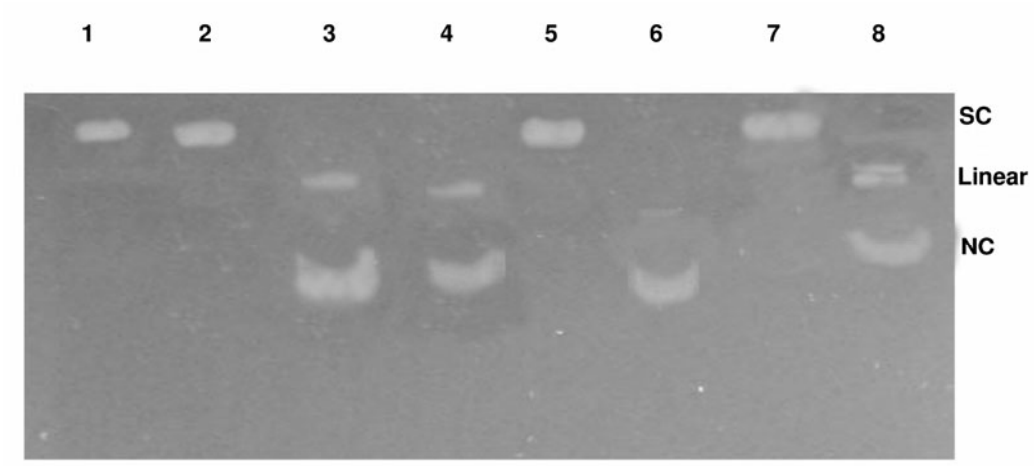

Fig. 9. Gel electrophoresis diagram showing the cleavage of SC pUC 19 DNA (0.2 μg) by the synthesized complexes (50 μM) in the presence of MPA (5 mM): lane 1, DNA control; lane 2, DNA + L^1 (50 μM); lane 3, DNA + $[CuL^1(dppz)]Cl_2$ + MPA; lane 4, DNA + $[CuL^1(dppz)]Cl_2$ + distamycin (50 μM) + MPA; lane 5, DNA + $[CuL^1(dppz)]Cl_2$ + DMSO (4 μl) + MPA; lane 6, DNA + $[CuL^1(dppz)]Cl_2$ + SOD (1U) + MPA; lane 7, DNA + L^2 + MPA; lane 8, DNA + $[CuL^2(dppz)]Cl_2$ + MPA.

experiments using MPA or the complexes alone do not show any apparent cleavage of SC DNA. To determine the groove selectivity of the complexes, control experiments were performed using minor groove binder distamycin. The addition of distamycin did not inhibit the cleavage for the complexes. This finding suggests major groove binding for the complexes. Control experiments show that the hydroxyl radical scavenger catalase or DMSO inhibits the DNA cleavage suggesting the possibility of hydroxyl radical and/or ''copper-oxo'' intermediate as the reactive species [30]. SOD addition did not have any apparent effect on the cleavage activity indicating the non-involvement of O^{2-} in the cleavage reaction.

Hydrolytic cleavage and ligation of the DNA linearised by zinc(II) complexes. To investigate the mechanism the DNA cleavage promoted by zinc complexes, hydroxyl radical scavenger, reductant and oxidant were introduced to the system. As shown in Fig. 10 and Supplementary, no evidence of inhibition of DNA cleavage is observed in the presence of scavengers, which suggests that hydroxyl radical, (3-mercaptopropionic acid and hydrogen peroxide) might not have occurred *via* an oxidative pathway but took place probably *via* a hydrolytic pathway. Further experiments support this assumption. It is well-known that in DNA hydrolytic cleavage 3′-OH and 5′-OPO_3 (5′-OH and 3′-OPO_3) fragments remain intact and that these fragments can be enzymatically ligated and end-labeled. Figure 10 and Supplementary File show that the linear DNA fragments, cleaved by zinc complex, can be relegated by T4 ligase just like the linear DNA mediated by E*co*R1. This implies that the process of DNA cleavage by the complex occurs *via* a hydrolytic path.

Photo-induced DNA cleavage study. Photo-induced DNA cleavage experiments were carried out in UV and visible light using the ligands and their copper complexes (50 and 100 μM) and SC pUC19 DNA (0.2 μg, 33.3 μM) in the presence and absence of various inhibitors. The DNA cleavage of ligand alone is inactive. The result indicates the importance of the metal in the complexes for observing the photo-induced DNA cleavage activity. All the complexes cleave the pUC19 DNA from its SC to NC form even in the absence of inhibitors on irradiation with UV light at 360 nm. The presence of singlet oxygen quencher, like sodium azide, inhibits the cleavage. An enhancement of photo-cleavage of DNA was observed in D_2O solvent in which $^1O_2$ had longer life time [31]. Hydroxyl radical scavenger DMSO or KI did not show any significant inhibition in the DNA cleavage activity. The results are indicative of the presence of a type-II in which the photo-excited complexes activate molecular oxygen from its stable triplet to the cytotoxic singlet state. Moreover, the results suggest the formation of singlet oxygen as the respective species in a type-II process in the metal-assisted photo-excitation process involving ligand n-π* and π-π* transitions (Fig. 11 and Supplementary). The proposed mechanistic pathway involved for the photo-induced cleavage of SC-DNA by complex is shown below:

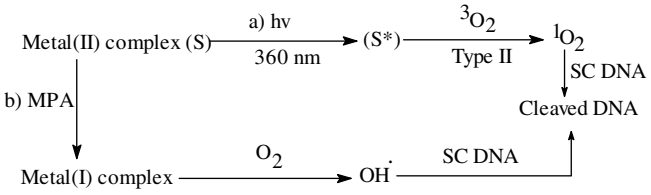

CONCLUSIONS

Novel copper(II) and zinc(II) complexes of the type $[ML(dppz)]Cl_2$, [L = Schiff base derived from the condensation of 3-(3-phenyl-allylidene)-pentane-2,4-dione and para substituted aniline; X = $-NO_2$ (L^1), -H (L^2), -OH (L^3) and $-OCH_3$ (L^4); dppz = dipyrido (3,2-a:2′3,′-c)phenazine] were synthesized and structurally characterized. They have adopted square-planar geometry around the central metal ion. The planarities, flexible and extended conjugation of the ligands containing substituted groups, have a profound effect on redox behaviour, DNA binding and cleavage activity of the complexes. Mechanistic investigations show a major groove binding for the synthesized complexes with DNA. Chemical nuclease activity of the synthesized copper complexes in the presence of a reducing agent, 3-mercaptopropionic acid *via* mechanistic pathway involves the formation of hydroxyl radical as the reactive species. Pathways involving singlet oxygen in the DNA photo-cleavage reactions have been proposed from the observation of the complete inhibition of the cleavage in the presence of sodium azide and enhancement

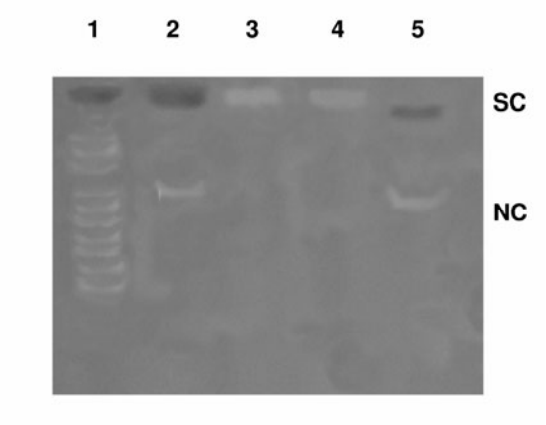

Fig. 10. Gel electrophoresis diagram for ligation of SC pUC 19 DNA linearized by zinc complexes: lane 1, DNA markers; lane 2, DNA + $[ZnL^1(dppz)]Cl_2$; lane 3, DNA + $[ZnL^1(dppz)]Cl_2$ + T4 DNA ligase; lane 4, DNA + $[ZnL^1(dppz)]Cl_2$ + EcoR1; lane 5, DNA + $[ZnL^1(dppz)]Cl_2$ + EcoR1 + T4 DNA ligase.

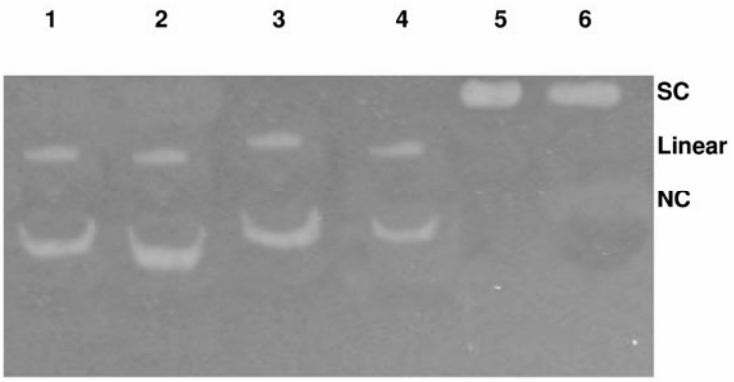

Fig. 11. Gel electrophoresis diagram showing the photocleavage of pUC 19 DNA by the synthesized complexes in the presence of various reagents irradiation with UV light of 365 nm: lane 1, DNA + $[CuL^4(dppz)]Cl_2$ (60 min); lane 2, DNA + $[CuL^1(dppz)]Cl_2$ + D_2O (14 µl); lane 3, DNA + $[CuL^4(dppz)]Cl_2$ + SOD (1 U); lane 4, DNA + DMSO (4 µl) + $[CuL^4(dppz)]Cl_2$ (30 min) lane 5, DNA + $[CuL^1(dppz)]Cl_2$ + sodium azide (100 µM); lane 6, DNA + $[CuL^2(dppz)]Cl_2$ + sodium azide (100 µM).

of cleavage in D_2O. Hydroxyl radical scavengers like DMSO do not show any significant effect on the DNA cleavage activity. These findings suggest the formation of singlet oxygen as the reactive species in a type-II process. The hydrolytic cleavage of DNA by the zinc complexes was supported by the evidence from free radical quenching and T4 ligase ligation.

ACKNOWLEDGEMENTS

The authors express their heartfelt thanks to the Department of Science and Technology, New Delhi, for financial assistance. They also express their gratitude to the Managing Board, VHNSN College, Virudhunagar, for providing research facilities.

SUPPLEMENTARY MATERIAL

Available from the corresponding author (Dr. N. Raman, Research Department of Chemistry, VHNSN College, Virudhunagar, India-626 001; E-mail: drn_raman@yahoo.co.in) C:\Documents and Settings\welcome\Desktop\Rev.JICS\Supplementary(Ms.No. IR-09-260-35).doc

REFERENCES

[1] S. Srinivasan, G. Rajagopal, P.R. Athappan, Trans. Met. Chem. 26 (2001) 588.

[2] K. Karaoglu, T. Baran, K. Serbest, M. Er, I. Degirmencioglu, J. Molecu. Str. 30 (2009) 39.

[3] L.-Z. Li, C. Zhao, T. Xu, H.-W. Ji, Y.-H. Yu, G.-Q. Guo, H. Chao, J. Inorg. Biochem. 99 (2005) 1076.

[4] D.S. Sigman, A. Mazumder, D.M. Perrin, Chem. Rev. 93 (1993) 2295.

[5] H.H. Hammud, G. Nemer, W. Sawma, J. Touma, P. Barnabe, Y. Bou-Mouglabey, A. Ghannoum, J. El-Hajjare, J. Usta, Chemico-Biol. Inter. 173 (2008) 84.

[6] B. Meunier, in: B. Meunier (Ed.), DNA and RNA Cleavers and Chemotherapy of Cancer and Viral Diseases, Kluwer, Dordrecht, The Netherlands, 1996.

[7] Y. Liu, T. Chen, Y.-S. Wang, W.-J. Mei, X.-M. Huang, F. Yang, J. Liu, W.-J. Zheng, Chemico-Biol. Inter. 183 (2010) 349.

[8] C.J. Burrows, J.G. Muller, Chem. Rev. 98 (1998) 1109.

[9] J. Chen, J. Stubbe, Nat. Rev. Cancer 5 (2005) 102.

[10] K.L. Hass, K.J. Franz, Chem. Rev. 109 (2009) 4921.

[11] B.R. James, R.J.P. Williams, J. Chem. Soc. (1961) 2007.

[12] J.E. Dickeson, L.A. Summers, Aust. J. Chem. 23 (1970) 1023.

[13] E. Amouyal, A. Homsi, J.-C. Chambron, J.-P. Sauvage, Dalton Trans. (1990) 1841.

[14] R.J. Angellici, Synthesis and Techniques in Inorganic Chemistry, W.B. Saunders Company, 1969.

[15] N. Raman, R. Jeyamurugan, B. Rajkapoor, V. Magesh, Appl. Organometal. Chem. 23 (2009) 283.

[16] J. Marmur, J. Mol. Biol. 3 (1961) 208.

[17] N. Raman, R. Jeyamurugan, A. Sakthivel, L. Mitu, Spectrochim. Acta 75A (2010) 88.

[18] J.B. Charies, N. Dattagupta, D.M. Crothers, Biochemistry 21 (1982) 3933.

[19] S. Satyanarayana, J.C. Daborusak, J.B. Charies, Biochemistry 32 (1983) 2573.

[20] H. Beinert, J. Inorg. Biochem. 44 (1991) 17.

[21] A.B.P. Lever, Inorganic Electronic Spectroscopy, Elsevier, Amesterdam, 1984.

[22] P. Banerjee, A. Company, T. Weyhermoller, E. Bill, C.R. Hess, J. Inorg. Chem. 48 (2009) 2944.

[23] R.K. Ray, G.B. Kauffman, Inorg. Chim. Acta 173 (1990) 207.

[24] N. Raman, R. Jeyamurugan, J. Coord. Chem. 62 (2009) 2375.

[25] P. Uma Maheswari, M. Palaniandavar, Inorganica Chim. Acta 357 (2004) 907.

[26] M.T. Carter, M. Rodriguez, A.J. Bard, J. Am. Chem. Soc. 111 (1989) 8901.

[27] H. Chao, W.J. Mei, Q.-W. Huang, L.-N. Ji, J. Inorg. Biochem. 92 (2002) 165.

[28] B. Peng, H. Chao, B. Sin, H. Li, F. Gao, L.-N. Ji, J. Inorg. Biochem. 101 (2007) 404.

[29] M.N. Patel, M.R. Chhasatia, S.H. Patel, H.S. Bariya, V.R. Thakkar, J. Enzy. Inhibi. Med. Chem. 24 (2009) 715.

[30] T.B. Thederahn, M.D. Kuwabara, T.A. Larsen, D.S. Sigman, J. Am. Chem. Soc. 111 (1989) 4946.

[31] R. Zhao, R. Hammitt, R.P. Thummel, Y. Liu, C. Turro, R.M. Snapka, Dalton Trans. (2009) 10926.